1.D.2 *Nuclear Physics* **A112** (1968) 204—208; © *North-Holland Publishing Co., Amsterdam*

EFFECTIVE MASS IN NUCLEI

G. F. BERTSCH and T. T. S. KUO
Palmer Physical Laboratory, Princeton University, Princeton, New Jersey †

Received 6 February 1968

Abstract: Core polarization renormalizes the single-particle strength by $\approx 25\,\%$ in intermediate and heavy nuclei. This produces a corresponding increase in the effective mass of particles near the Fermi surface.

1. Introduction

In the nuclei near the closed shells, the single-particle levels which are seen are well accounted for by calculation for a free particle in a potential well. For light nuclei, such as ^{41}Ca, there are enough well parameters to fit all the levels, but for heavier nuclei, such as ^{61}Ni, ^{209}Bi and ^{209}Pb, there are sufficient levels to provide a test of the potential well model.

If there is any systematic trend, it is that the Woods-Saxon well calculations tend to give levels too far apart [1]). For example, the calculation of Blomqvist and Wahlborn [2]) gave only three bound single-particle levels in ^{209}Bi whereas experimentally there are five. However, all the Bismuth levels are nicely fitted in a recent Woods-Saxon calculation [3]).

It might be hoped that the calculation could be improved by using a Hartree-Fock potential. Unfortunately a potential which gives saturation must put the occupied single-particle levels further apart than a local potential does. [4]) This is shown in nuclear matter calculations, which give an effective mass of about 0.7 near the Fermi surface [5]). The effective mass is required to be less than one at energies much larger than the Fermi energy, because of the short-range repulsion in the nucleon interaction.

There is then a problem to understand the success of the Woods-Saxon calculations: why is the effective mass near to one near the Fermi surface, when it is known to be smaller both above and below? A similar problem occurred in the study of liquid ^{3}He, and was successfully explained by coupling virtual excitations of the Fermi sea to the particles near the Fermi surface [6,7]). The problem of particle-phonon coupling is discussed in general in ref. [8]), where it is shown that there is always a positive contribution to the fermion effective mass, which decreases as the particle is moved away from the Fermi surface. It is well known from the theory of superconductivity that the single-particle levels are more closely spaced near the Fermi surface, although here

† This work was supported by in part the U.S. Atomic Energy Commission and the Higgins Scientific Trust Fund.

of course there is an energy gap producing completely different behavior in other respects.

Schrieffer has considered the formalism of coupling particles to collective particle-hole excitations for the nuclear structure problem [9]). This coupling to the low-lying collective excitations produces a significant depletion of the single-particle strength in light nuclei [10]) but apparently makes a negligible perturbation on the single-particle levels in heavy nuclei [2]). On the other hand, Brueckner and collaborators found a substantial effect from the very high energy excitations [11,12]). We shall compute the effective mass in finite nuclei by summing over all possible particle-hole states of low excitation energy and neglect completely the collective shifts on the energies. This appears to be reasonable because the collective states exhaust only a fraction of the total strength. Also, the $T = 0$ and $T = 1$ collective states are shifted in opposite directions, making some compensation.

2. Theory

In second-order perturbation theory there are two graphs contributing to the single-particle energy

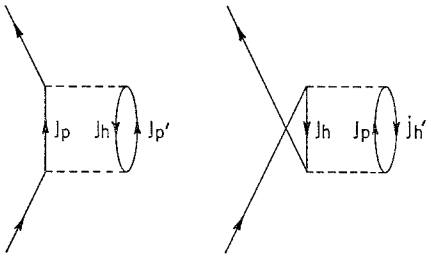

Fig. 1. Second-order contributions to the single-particle energy.

The first is a polarization of the core which lowers the energy of state j_1 by

$$\sum_{-} = -\sum_{J} \frac{2J+1}{2j_1+1} \frac{\langle (j_1 j_h)^J | V | (j_p j_{p'}) \rangle^2}{\varepsilon_{j_p} + \varepsilon_{j_{p'}} - \varepsilon_{j_h} - \varepsilon_{j_1}} \tag{1}$$

as in ref. [11]). The factor $(2J+1)/(2j_1+1)$ weighs the interactions so that there are $(2j_h+1)$ interactions all together, corresponding to the number of core particles. The other graph is in interference with a ground-state correlation and so decreases the binding of the state j_1. The energy perturbation is

$$\sum_{+} = \sum_{J} \frac{2J+1}{2j_1+1} \frac{\langle (j_1 j_p)^J | V | j_h j_{h'})^J \rangle^2}{\varepsilon_{j_1} + \varepsilon_{j_p} - \varepsilon_{j_h} - \varepsilon_{j_{h'}}} \,. \tag{2}$$

If two orbitals are identical so that not all J are represented in a given T state an extra factor of 2 may be required.

In a pairing model, only the second graph would contribute, through the $J = 0$, $T = 1$ matrix element. Although this matrix element is strong, it does not have much weight, and in fact more than $\frac{2}{3}$ of the strength near closed-shell nuclei comes from the $T = 0$ interaction.

For a qualitative discussion of the behavior of these graphs we sum over V^2 and use an average energy denominator. Neither of these quantities depends very much on the initial single-particle wave function, at least for an infinite system. If energies are measured from the Fermi energy, there should even be approximate equality between the 2p-1h and 1p-2h excitation energies:

$$E_x \approx \overline{\varepsilon_{j_p}+\varepsilon_{j_{p'}}-\varepsilon_{j_h}} \approx \overline{\varepsilon_{j_p}-\varepsilon_{j_h}-\varepsilon_{j_{h'}}}.$$

The total energy shift is then

$$\Sigma \approx -\frac{\sum V^2}{E_x-\varepsilon_{j_1}} + \frac{\sum V^2}{E_x+\varepsilon_{j_1}}.$$

To see how this gives an effective mass, we write

$$\varepsilon = \varepsilon_0+\Sigma(\varepsilon)$$

and expand $\Sigma(\varepsilon)$ in powers of ε to get

$$\varepsilon = \frac{\varepsilon_0+\Sigma_0}{\left(1-\dfrac{\partial\Sigma}{\partial\varepsilon}\right)} = \frac{m}{m^*}(\varepsilon_0+\Sigma_0).$$

The above expression for Σ when expanded is

$$\Sigma \approx 0-2\left(\frac{\sum V^2}{E_x^2}\right)\varepsilon_j+\ldots.$$

At the Fermi surface in a normal system the two contributions to Σ just cancel †. The interference graph alone would give an energy gap. As the particle moves away from the Fermi surface, the attractive polarization graph increases and the repulsive interference graph decreases, giving an effective mass

$$\frac{m}{m^*} - 1 = \sum_{pp'h}\frac{V^2}{(E_x-\varepsilon_j)^2} + \sum_{php'}\frac{V^2}{(E_x+\varepsilon_j)^2}$$
$$\approx 2\,\frac{\sum V^2}{E_x^2}. \qquad (3)$$

This is also approximately equal to the depletion of the single-particle strength of the state [10]). At energies $\varepsilon_j \approx E_x$ the contributions to the polarization graph are not of

† This will happen in the schematic calculation of ref. [10]) if the dependence of the force on the angular momentum of the single particle states is taken into account.

the same sign, and this source of an effective mass enhancement disappears. From the Pb computation we find $E_x \approx 15$ MeV. This give the scale of energy where the effective mass enhancement is operative.

3. Brueckner theory

The matrix elements we use contain short-range correlations of the Brueckner-theory. A problem arises, that some of the correlations may be counted twice, once in the Brueckner theory G matrix which is used in the "Hartree-Fock" potential, and again in this explicit calculation. However, the Brueckner correlations are high in energy, of the order of 150 MeV in the approximations used. This happens because the low-energy correlations are damped with an artificial energy gap. Therefore there should be a small overlap between the Brueckner correlations and the ones considered here.

Also, the short-range correlations give a single-particle strength depletion of the order of 15 %. The effect from low energy excitations is considerably larger, of the order of 25 %, so it is clear that proper counting will not change the result very much.

Brown and Wong [14]) considered the problem of double counting in detail for ^{16}O and found the error to be small.

4. Results

The matrix elements for the nucleon interaction in the calcium region and the lead region were calculated from the Hamada-Johnston force, using the same techniques as in ref. [13]). With these matrix elements and a constant energy denominator of 21 MeV, the self-energy graphs of ^{41}Ca were computed according to eqs. (1) and (2). The results are shown in table 1. Since the energy denominator was taken as constant there should be no variation of Σ with orbital. This is roughly the case. The other qualitative feature from Fermi-liquid theory, that the two graphs should cancel, is true to the same extent. The effective mass enhancement derived from this according to eq. (3) is 23 %. This may be seen from the table by adding the absolute values of the two contributions to the self energy of the $f_{\frac{7}{2}}$, and dividing by 21 MeV, the energy denominator.

We have also calculated for particle orbitals in the Pb region. In this case, we took empirical single-particle energies wherever possible, and $\hbar\omega = 7.0$ MeV otherwise. All excitations to ≈ 25 MeV were included; this involves $0\hbar\omega$, $2\hbar\omega$ and some $4\hbar\omega$ excitations. As may be seen from table 2, the ε_j dependence of both graphs is quite obvious. The effective mass derived for proton orbitals according to eq. (3) is 32 %, and for neutron orbitals 15 %. The difference appears to be due to the neutron excess which correlates with a valence proton better than a valence neutron.

TABLE 1

Second-order contributions to single-particle energy in ^{41}Ca, calculated with the Hamada-Johnston potential and reaction-matrix techniques (E_x = 21 MeV for all four orbitals)

Orbital	polarization graph	g.s. correlation graph
$f_{\frac{7}{2}}$	−2.94	1.90
$p_{\frac{3}{2}}$	−3.10	1.64
$f_{\frac{5}{2}}$	−3.43	2.56
$p_{\frac{1}{2}}$	−3.27	1.76

TABLE 2

Second-order contributions to single-particle energies for Pb orbitals, using empirical single-particle energies

Orbital		polarization graph	g.s. correlation graph
proton	$h_{\frac{9}{2}}$	−3.2	1.8
	$f_{\frac{7}{2}}$	−3.2	1.4
	$i_{\frac{13}{2}}$	−3.3	1.9
	$f_{\frac{5}{2}}$	−4.7	1.2
	$p_{\frac{1}{2}}$	−3.9	1.0
	$p_{\frac{3}{2}}$	−5.2	1.0
neutron	$g_{\frac{9}{2}}$	−0.8	1.1
	$i_{\frac{11}{2}}$	−1.7	1.6

5. Conclusion

The recent Woods-Saxon calculation [3]) of Pb levels shows no such difference between neutrons and protons. It must be remembered, however, that the Hartree-Fock part of the potential has not been included, and would be sufficiently non-local with the reaction matrix elements [13]) to counterbalance the enhancement found above. It would be reasonable to expect that it would be more non-local for protons than for neutrons at the Fermi surface, so that the net change in effective mass would be close to zero for both kinds of particles. At any rate there is consistency with experiment, considering the theoretical uncertainties in the Hartree-Fock potential.

We would like to thank G. E. Brown for thought-provoking discussions on the topic.

References

1) G. E. Brown, J. H. Gunn and P. Gould, Nucl. Phys. **46** (1963) 598
2) J. Blomqvist and S. Wahlborn, Ark. Fys. **16** (1960) 545
3) E. Rost, Phys. Lett. **26B** (1968) 184
4) V. F. Weisskopf, Nucl. Phys. **3** (1957) 423
5) K. A. Brueckner and J. L. Gammel, Phys. Rev. **109** (1958) 1023
6) N. F. Berk and J. R. Schrieffer, Phys. Rev. Lett. **17** (1966) 433
7) S. Doniach and S. Engelsberg, Phys. Rev. Lett. **17** (1966) 750
8) A. Abrikosov, L Gorkov, I. Dzyaloshinski, Methods of quantum field theory in statistical physics, Sec. 21
9) J. R. Schrieffer, Nucl. Phys. **35** (1962) 363
10) G. E. Brown, J. A. Evans and D. J. Thouless, Nucl. Phys. **45** (1963) 164
11) K. A Brueckner, J. L. Gammel and J. T Kubis, Phys. Rev **118** (1960) 1438
12) B. H. Brandow, Phys. Lett. **4** (1963) 8, 152
13) T. T. S. Kuo and G. E. Brown, Nucl. Phys. **85** (1966) 40
14) G. E. Brown and C. W. Wong, Nucl. Phys. **A100** (1967) 241